

Non-Destructive Test Application in Civil Infrastructure

Murad Al Qurishee¹, Weidong Wu², Babatunde Atolagbe³, Said El Said⁴, Arash Ghasemi⁵

¹Graduate Transportation Associate, Tennessee Department of Transportation

²Associate Professor, University of Tennessee at Chattanooga

³Transportation Engineer, Maryland Department of Transportation

⁴Civil Engineering Manager, Tennessee Department of Transportation

⁵Director, Civil Infrastructure Laboratory & Research, University of Tennessee at Chattanooga

Abstract - Structural strength assessment of civil infrastructure is a prior concern to engineers. This paper presents laboratories study as well as on site study data analysis gathered by many authors and critical review of existing nondestructive testing (NDT) methods. The techniques considered are ultrasonic pulse velocity method, surface hardness method, penetration resistant method, pullout test, the impact-echo system, infrared thermography, ground penetration radar, ultrasonic methods, acoustic emission method, maturity method, stress wave propagation method, corrosion potential test, X-ray computed tomography, Electrical Impedance Spectroscopy (EIS), and Wireless sensor network. Applications, advantages, accuracy, limitations, instrumentation, principles, and ASTM standard of these techniques are discussed for the infrastructural condition assessment.

Key Words: ultrasonic pulse velocity method; surface hardness method; penetration resistant method; pullout test; the impact-echo system; infrared thermography; ground penetration radar; ultrasonic methods; acoustic emission method; maturity method; stress wave propagation method; corrosion potential test; X-ray computed tomography; Electrical Impedance Spectroscopy (EIS); Wireless sensor network.

1. INTRODUCTION

Nondestructive evaluation of concrete strength is required in various contexts, such as evaluating whether there is damage developed over time or knowing new requirements in structure due to change in regulations or load conditions. NDT techniques offer an indirect approach towards material mechanical properties and help decision making regarding maintenance [1, 2]. The highest requirement for assessment of concrete is to quantify mechanical properties like strength and the lowest one is detecting or ranking the damages [3].

Due to scarcity of available funds, the state agencies are looking for cost efficient, rapid, and reliable condition assessment methods for public safety. Researchers have been devoted to synthesizing the NDT abilities regarding given problems [4-7], to data processing or development of NDT for better assessment of infrastructure, or to defining the most promising paths for development.

To know the suitability of the proposed NDT techniques, it is advisable to take a feasibility study on the structure for the investigation of structural problems. This procedure is called 'Desk study' [8].

There are five major factors that influence the success of an NDT survey [9]:

1. Penetration depth into the structure.
2. Lateral and vertical resolution for anticipated target problems.
3. Comparison of target and its surroundings for physical properties of the structure.
4. Signal to noise ratio of the investigated structure for the physical property's measurement
5. Historical information of the structure about the construction methods of the structure.

2. OVERVIEW OF NON-DESTRUCTIVE METHODS

2.1 Ultrasonic pulse velocity method

Ultrasonic pulse velocity method (UPV) and rebound measurement method are the most widely used methods for concrete strength assessment [10, 11]. The method measures the longitudinal pulse wave (20 to 150 kHz commonly) travel time through the concrete. Between the initial onset and reception of pulse wave, an electronic device measures the required travel time. ASTM C 597 described the standard procedure and apparatus.

There are three types of UPV methods: direct transmission (cross probing), semi direct transmission, and indirect transmission (surface probing) [12] as shown in fig.2. Fig.1 shows the ultrasonic pulse velocity meter and the schematic diagram of UPV.

Applications of UPV:

1. Evaluation of concrete homogeneity and dynamic elastic modulus.
2. Inspection of prestressed and precast beams, new and old structure, fire damaged areas, columns, slabs, concrete forms and other structures.

3. Detection of voids, honey combs, cracks and other non-homogeneous condition of the concrete.
4. PULSONIC model 58-E4900 combined with oscilloscope can do Spectrum analysis by FFT method, evaluation of concrete strength by SonReb method incorporated with concrete hammer.

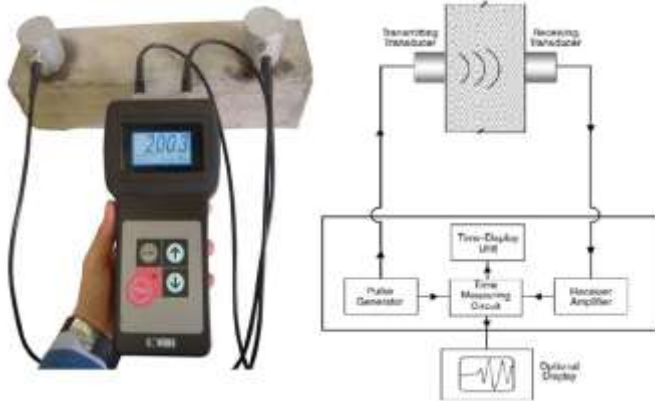


Figure 1: Ultrasonic pulse velocity tester (58-E4800 UPV tester) (left) [13]; pulse velocity test schematic diagram [14]



Figure 2: Different UPV methods and bridge girder testing by direct transmission method [15].

The velocity of ultrasonic waves in concrete shows a significant increase after casting of concrete in first days, and this is the basic reason for using UPV in concrete strength assessment. But after 5 to 7 days of the casing, the sensitivity of UPV to the rate of concrete strength is considerably lower than the first few days [16]. There are many other factors which affect both UPV and concrete strength quantified by many authors [11, 17-24] as described below.

1. Aggregate percentage and type have high influence, and aggregate size has an average influence on UPV. Depending on type and density of aggregate in undamaged rocks UPV can vary more than 6000 m/s to less than 4000 m/s, and a common change in concrete is 400 m/s [25, 26].
2. Cement percentage and type have a moderate influence on UPV. Water cement ration has high influence, and fly ash content has an average influence on UPV [27].
3. Humidity is another higher influencing factor. Between air and saturated condition of concrete the pulse velocity may increase up to 5% [28].
4. Rebars in the concrete offer a higher velocity by proving an easier path for wave propagation. It is recommended that measure UPV where the rebar influence is neglected [27].

5. Between 0° c and 30° c temperature influence is neglected, but for hot or cold weather the influence is noted [27].
6. All types of defects, voids, and cracks have a higher influence on UPV because wave propagation is affected by concrete cracks. There is an average influence of age on UPV.

The method has these following limitations:

1. If the factors data as discussed above are not available, assessment of concrete compressive strength by UPV provides 95% confidence level which is 15% to 20% depending on concrete mix design data available.
2. For better results with both the new and old structures, the methods need the incorporation of concrete hammer methods.

2.2 Surface hardness method

Concrete strength is judged by its compressive strength which affects load bearing capacity and durability of the concrete structure. The Schmidt rebound hammer is the most widely used portable NDT instruments to measure surface hardness of concrete. Ernst O. Schmidt developed this test hammer in 1950. Schmidt OS-120 hammer is recommended for 1 to 10MPa compressive strength range concrete. For 10 to 100MPa compressive strength concrete Silver Schmidt hammer is recommended. Fig. 3 shows Schmidt OS-120 and Silver Schmidt hammer.



Figure 3: Schmidt OS-120 (left) [29]; Silver Schmidt hammer (right) [30]

First, the extended plunger is placed at the surface of the concrete (fig. 4 (a)). The internal spring is extended when the outer body of the hammer is pressed on the concrete surface (fig. 4 (b)). When the spring is fully extended, the latch is released and the hammer impacts on the surface of the concrete wall (fig. 4 (c)). On the plunger, the hammer impacts upon and along a guide-scale with the spring-controlled mass rebound taking a ride which provides hammer rebound number (fig. 4 (d)). In ASTM C 805 [31], standard procedure for rebound hammer number has been established. HAMMER LINK Proceq software offers the rebound number computation platform.

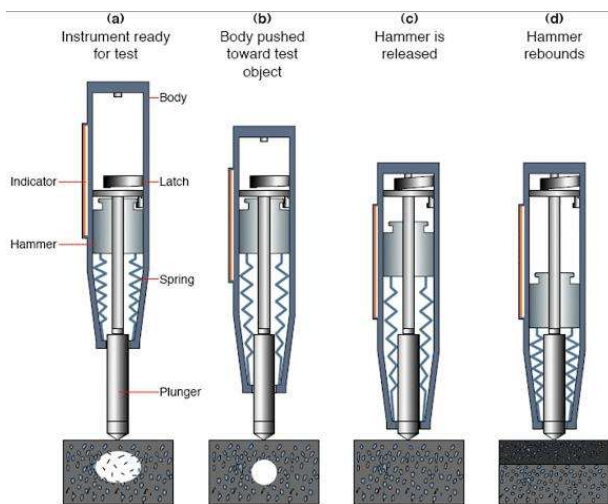


Figure 4: Schematic diagram operation of rebound hammer [32].

Inexpensive, quick and user-friendly hammer surface harness method depends on the following parameters [33]:

1. The type and amount of aggregate are a critical issue between the rebound number and strength.
2. The strength-rebound calibration is affected by wet surface. There is a lower bound number in wet surface than with dry surface. Wet surface underestimates up to 20% of concrete strength [28].
3. Surface carbonation is hard, and it increases the rebound number. Carbonation is evident in old structures. In carbonated surfaces, it is recommended that the carbonation layer be removed in a small area and the results obtained from the area be compared with the rest of the structure.
4. Location of plunger over a stiff aggregate yields a high bound number while the location of plunger over a large void or a soft aggregate yields a lower bound number. According to ASTM C 805 guideline, 10 measurements should be taken for a test. If reading deviates more than 7 units from the average, the reading is disregarded, and the entire measurement is disregarded if there are two measurements which deviate more than 7 units from the average.

In practice, it is difficult to make a good correlation between rebound number and strength based on all parameters. With a properly calibrated laboratory specimen the accuracy of estimating concrete strength is ± 15 to 20 percent, and it is ± 25 percent for a concrete structure [10].

2.3 Penetration resistant method

The Windsor HP Probe system is used to drive a metal rod energized by a sudden charge of powder (explosive). From the depth of penetration, the device estimates the concrete strength. The concrete compressive strength is inversely proportional to the depth of penetration. The Windsor Probe can measure maximum 110MPa concrete compressive strength.

The system consists of three probes of 0.25" diameter and length 3.125". Cartridge and other related equipment are shown in fig 5. When fired, the powder produces 575 lbs ft energy to drive probe into the concrete.

A 7-inch equilateral triangle locating template is used to position three probes at each corner. The penetration depth is calculated from the exposed length from the surface of the concrete using a calibrated depth gauge as shown in fig. 6. From charts of compressive strength verses, penetration for aggregate hardness between 3 - 7 on Moh's scale, the compressive strength of concrete can be evaluated from a field penetration depth as shown in fig. 7. ASTM C 803 described the standard test procedure [34].



Figure 5: Windsor Probe instruments (left) [35]; equilateral triangle locating template used to positioning probes (middle) ; three probes at each corner (right) [36].

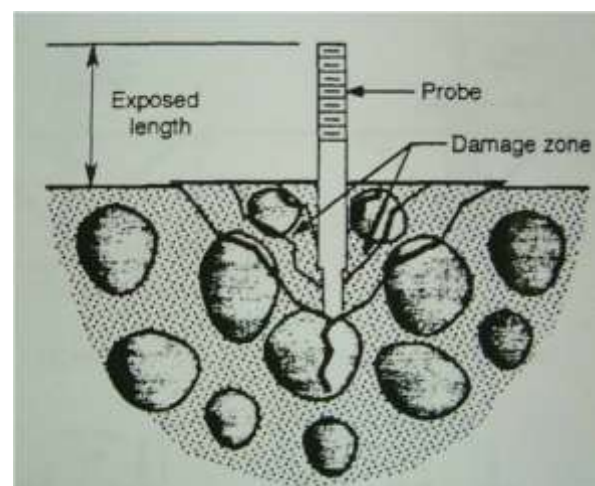


Figure 6: Probe penetration test conical failure [37]

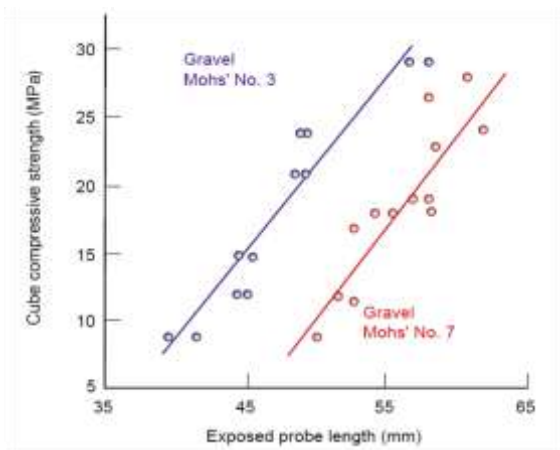


Figure 7: compressive strength versus penetration for aggregate hardness between 3 - 7 on Moh's scale [37]

Though Windsor Probe test is costly compared to surface hammer test, it is superior to hammer test because it measures not only surface hardness but also concrete internal hardness. It is an excellent method for determining the stripping time for formworks. The type and amount of aggregate play a key role in determining penetration depth. Soft aggregate (lower Mohs' scale) allows greater penetration than hard aggregate (higher Mohs' scale). The variation in data in Windsor Probe test is higher than the surface hardness method.

2.4 Pullout Test

A pullout test measures the force required to pull out a special steel bar embedded in the fresh concrete. The principle behind the test is that the concrete strength is proportional to the force required to pull out the steel bars. From pull out force vs compressive strength graph (fig. 10), the concrete compressive force is calculated. A complex three-dimensional stress state is developed inside the concrete during the test as shown in fig. 9. The failure criteria include compressive strength of concrete, the interlocking of aggregate around the circumferential of crack, and concrete fracture toughness. The pull-out strength depends on the arrangement of the embedded insert, dimension of bearing ring, depth of embedment and type of aggregate in the concrete. ASTM C 900 describes the standard test procedure [38]. Fig.8 shows the pullout testing instruments (latest model: Hydrajaws 2050 Deluxe).

The test provides practical results for determining the optimum time of safe form-stripping, determining concrete strength for carrying out post-tensioning, and evaluating of curing period based on target strength. As larger volume and greater depth of concrete are involved in this test, this test is superior to hammer and penetration test [39]. But the limitation of this test is that it does not provide the statistical procedure to measure other strength properties. The steel rod must be embedded in during the pouring of concrete and hence the test cannot be undertaken

at later ages. As it pulls out a concrete portion, repair is required after the test.



Figure 8: Hydrajaws 2050 Deluxe (left); Hydrajaw Model 2000 Deluxe pull tester with Bluetooth technology (Right) [40].

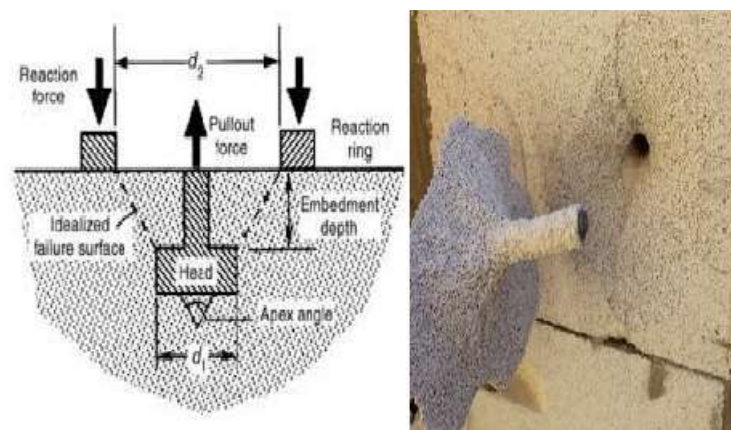


Figure 9: Schematic diagram of pull out test of concrete (left) [41]; triangular pull out concrete [42]

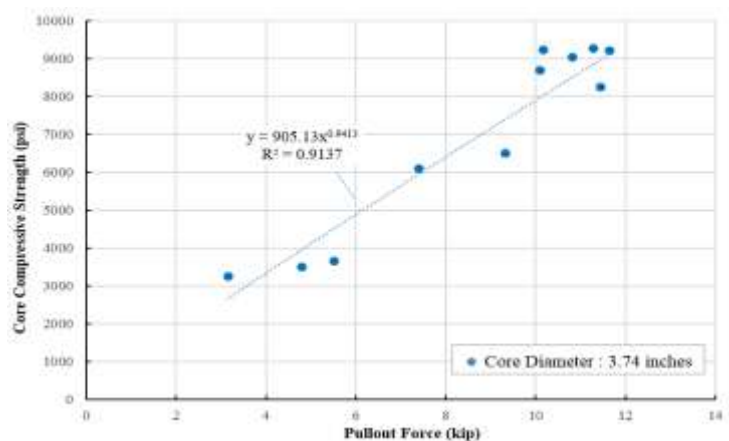


Figure 10: Pull out correlation with concrete compressive strength.

2.5 The impact-echo system

The impact-echo system method measures concrete thickness and integrity from one surface. A small mounted hammer and an accelerometer mounted adjacent to the impact location are used to hit the surface of an investigated

structure and record the reflected energy respectively as shown in fig. 11. A voltage proportional to displacement is produced by the piezoelectric transducer and transferred to a computer memory. Then fast Fourier Transform (FFT) is used to analyze frequency domain signal and a frequency response function (FRF) is calculated from the impulse hammer system. The slab or wall thickness can be found from the depth of the reflector. ASTM C 1383 describes standard procedure for the impact-echo system.

The impact-echo consists of spherical impactors, analog to digital data acquisition systems, a hand-held transducer unit, a computer, and a software package as shown in fig. 12 (left).

Impact-echo method is successfully used to detect

1. Basement wall and marine spun piles honeycombing.
2. Prestressed beams and slabs tendon ducts voids.
3. Retaining wall thickness.
4. Metal and concrete bonds in railways ties.
5. Flaws in the plate-type structure such as garage slabs, plaza deck slabs, and foundation walls.

Martin et al. found minimum resolution is half wavelength, $\lambda/2$ from an investigation of post-tensioned concrete bridge beams. To identify voided ducts in post-tensioned bridge beams, the resolution concept of $\lambda/2$ provides a good correlation between FE models and a laboratory experiment [43].

Davis et al. (1974) first used the FRF in concrete piles [44]. National Institute of Standards and Technology, USA (NIST) and Cornell University modernize the impact-echo system [45-47].

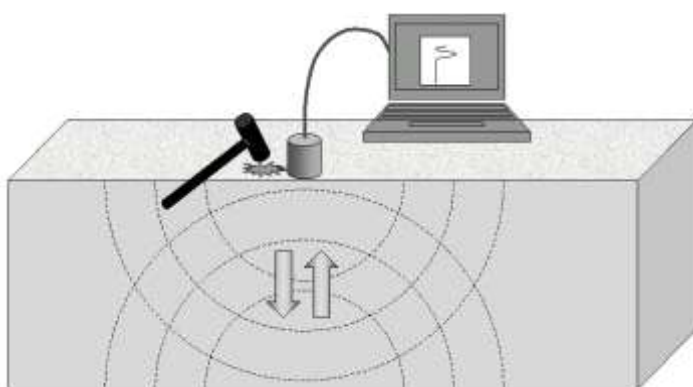


Figure 11: Back and forth propagation of compression wave generated from a hammer (left) [48].



Figure 12: Impact-echo instruments (left) [49]; impact-echo testing on a slab [50]

2.6. Infrared thermography

Sound concrete thermal properties are different from imperfection and high porosity localized zones. A thermal anomaly is present in the concrete structure temperature distribution when there are voids and imperfections in the concrete body. Malhotra et al. (2003) suggested that a good thermography can be obtained two or three hours after sunrise or sunset because at this time best thermal contrast can be obtained [10]. On a hot day, the heat flows inward, and temperature rises at the upper region of concrete flaw because the flaw does not conduct heat well. Similarly, on a cold night, the temperature drops on the upper region of concrete flaw compared with other portions of the structure as shown in fig. 15. Khan et al. (2015) developed heat transfer model for partially grouted concrete masonry walls [51].

The standard procedure for detecting cavities of frame buildings, wet insulation in roofing systems, delamination in bridge decks, air leakage site detection in building, and examining electrical and mechanical equipment are described in ASTM C1060, ASTM C1153, ASTM D4788, ASTM E1186 and ASTM E1934 respectively. Fig. 13 shows the FLIR infrared thermography camera (model: InGaAs SWIR Camera: A6200sc), and fig. 14 shows the difference between the standard camera and the infrared camera.



Figure 13: Infrared thermography camera (InGaAs SWIR Camera: A6200sc) [52]



Figure 14: Standard camera vs infrared camera [53]

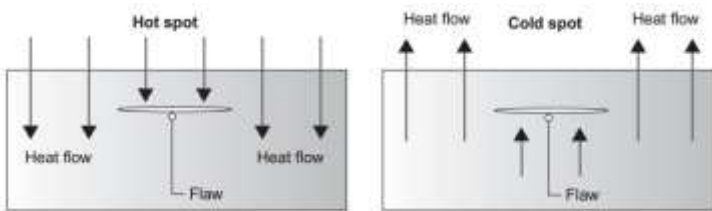


Figure 15: Anomaly temperature distribution due to presence of flaws in concrete slab [33]

Advantages of thermography [54]:

1. No need for contact between investigated structures and the camera. Thermography allows measurements of potentially hazardous areas because the range of distance between the object and the camera can be a few millimeters to kilometers.
2. The camera can monitor temperature of many points of a structure at a time.
3. Obscured objects can also be detected by infrared thermography because thermal radiation can penetrate mist and smoke easily.
4. The system can be altered to suit the target investigation by altering camera lens aperture and introducing various filters. The system is operable within a broad range of temperature -20 to 1600 °C.
5. Data manipulation can be done on a standard PC imaging software.
6. The imaging equipment is lightweight and easy to transport. The system is capable of monitoring rapid temperature fluctuations with an accuracy of ±0.08 °C.

Application of thermography:

1. Tunnel seepage identification as shown in fig. 16 [55].
2. Moisture detection on the surface [56].
3. Finding the source of stress location [57].

4. Deeper voids, crack detection as well as qualitative and quantitative applications in cultural heritage and civil engineering structures [58].
5. Buried water pipe leakage detection [59].
6. To detect heat losses, missing or damaged thermal insulation in walls and roofs, thermal bridges, air leakage and moisture sources in building [60-65].
7. Assessment of concrete deterioration due to rebar and prestressing strands corrosion [66].



Figure 16: water seepage detection in tunnel [67]

2.7 Ground penetration radar

Ground penetration radar (GPR) is a nondestructive rapid method using electromagnetic (EM) energy to probe subsurface. GPR antenna transmits EM waves into the structures, and GPR receiver receives the subsurface structures that reflected the signal. A portion of signal travels through the next layer until it diminishes, and the rest of the signal reflected from any reflector such as rebar or anomaly is received by the antenna. The reflected energy to the surface is a function of the electromagnetic impedance contrast of the two materials; the stronger GPR reflection comes from greater electromagnetic impedance. Ground-coupled and Air-coupled are two implementations of GPR as shown in fig. 17. Air-coupled GPR suspended typically 1 to 2ft above the ground, and some portion of the trace represents the travels of EM through the air. ASTM D6087 – 08 describes asphalt-covered concrete bridge decks evaluation standard test by GPR [68].



Figure 17: Ground-coupled GPR (left); Air-coupled GPR (right) [4]

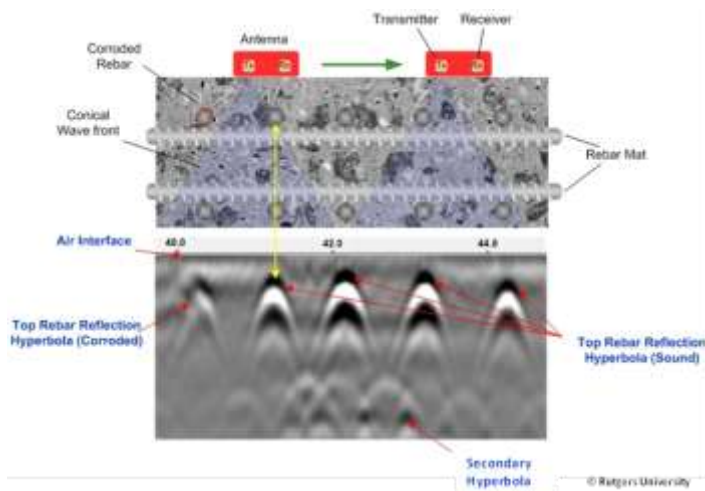


Figure 18: Rebar location by GPR [4]

GPR signal is attenuated in corroded concrete deck, moisture, and free chloride ions conductive materials. The phase velocity of GPR signal depends on the relative dielectric constant of the materials. The dielectric constant for air and water are 1 and 80 respectively. The relative dielectric constant is a function of porosity, water content, temperature, mix proportions, pore fluid solution, and particle shape. For example, moisture content in gravel increases the dielectric constant from 5 to 20. When rust is formed over a steel bar or delamination occurs by steel bar corrosion, electrical conductivity and dielectric properties of corroded rebar changes compared to sound rebar. As a result, velocity and amplitude of the reflected wave are changed compared to sound one. Fig. 19 shows GPR radiogram for a partially corroded steel bar.

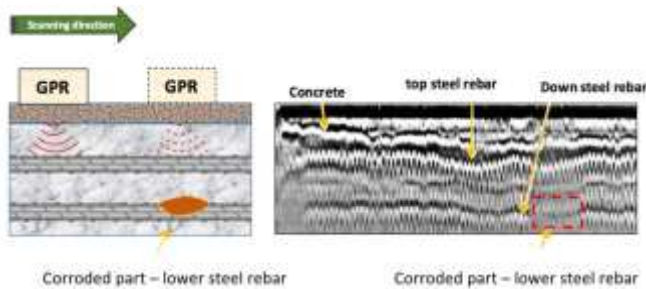


Figure 19: Corrosion detection by GPR [69]

Advantages of GPR over other NDT methods:

1. Rapid, reliable, repeatable, and well-established data acquisition method.
2. Well correlated between corrosive environment and electrical resistivity.
3. The method is popular to detect voids and delamination, rebar location (as shown in fig. 18) and arrangement, material interface changes and pavement thickness.

Limitation of GPR:

1. Expert people need data acquisition, processing, and interpretation.
2. It is costly when applied for an individual structure.
3. Signal penetration is attenuated when de-icing agent is used on the structure.
4. In extremely cold condition there is negative data.
5. Within the upper half of the deck, GPR can easily identify the corrosive rebar, but for lower half, it is difficult to detect due to upper half rebar mat.
6. Deck delamination cannot assess directly by GPR.
7. GPR signal attenuated due to conductive soil, wet clay, saltwater saturated water, etc.

2.8 Ultrasonic methods

Ultrasonic methods refer to propagation and reflection of the ultrasonic wave through a medium. There are five most popular ultrasonic methods: sonic tomography, sonic transmission method, sonic reflection method, sonic resonance method and ultrasonic method.

3.1.1. Sonic transmission method

In this method, a force hammer is used on one side of the investigated structure with a compressional frequency between 500Hz to 10 kHz, and on the opposite side an accelerometer is used to receive the frequency. The resulting wave velocity comes from the average of local velocity along the path as shown in fig. 20 (a). This method is called direct transmission modes, and it is useful for simple evaluation of the concrete walls of a masonry arch bridge [9].

The indirect transmission method is used to detect voids existence, estimate material uniformity, evaluate the depth of crack, calculate compressive strength and help in tomographic surveys. Sonic waves become attenuate and take longer time in transit of signal when it propagates through the crack, void or delamination at the interface between aggregate and mortar. Fig. 20 (b) and 20 (c) show the indirect transmission modes [9].

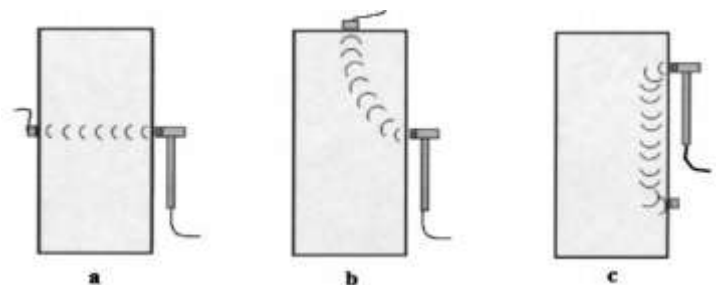


Figure 20: (a) direct sonic wave transmission mode; (b) semidirect transmission mode; (c) indirect transmission mode [9]

3.1.2. Sonic tomography

Seismic tomography is performed in direct mode as well as an oblique path along the wall surface. There are ray paths between the sonic source and receiver which crossed the masonry wall in a dense format. Each ray path represents a specific travel time between receiver and source. There was a Sonic tomographic survey on North Middleton Bridge as shown in fig. 21. The readings data were collected from downstream, upstream and under the arch of the abutment. A total of 142 straight rays were made from 15 stations at level 2m of the grid as shown in fig. 22. The output result as shown in fig. 4 demonstrated that the high-velocity areas along the wall represent the stone masonry and medium to low-velocity areas towards the center of the plot represent the backfill materials as shown in fig. 23. High-velocity areas along the upstream and especially downstream areas represents a continuous homogeneous dense material. After endoscopic investigation, the dense materials revealed to be cement grouted zones [70]. Tomographic survey associated with ultrasonic gives a better understanding of the bridge structure [43].

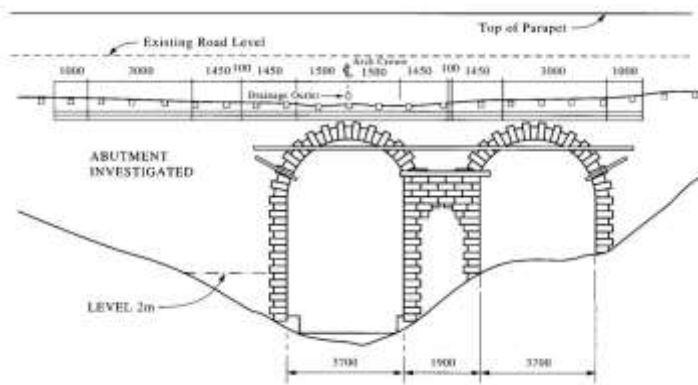


Figure 21: North Middleton bridge [70]

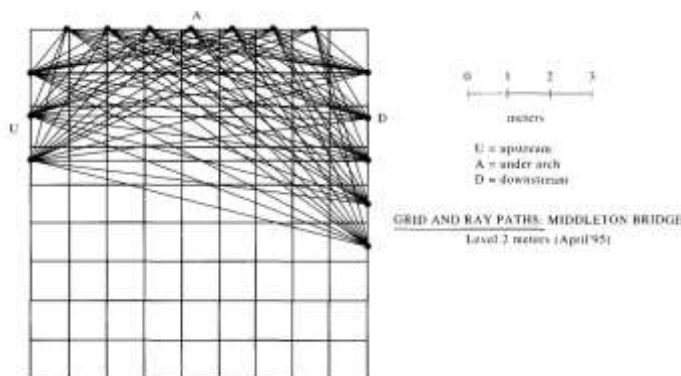


Figure 22: Densely ray paths between the sonic source and receiver [70]

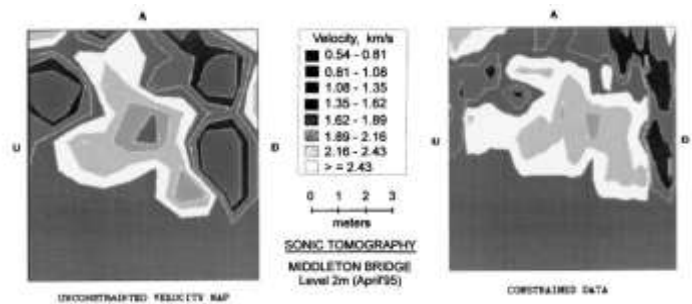


Figure 23: Reconstruction of sonic tomographic [70]

3.1.3. Sonic reflection method

In this method, both sonic wave source and receiver are on the same face of the masonry wall as in case of indirect transmission. The recorded stress wave comes from the reflection of the wave from any internal flaws or the rear face of the investigated structures. The velocities coming from the rear face or face of a structure indicates the local velocity along the path. The sonic reflection method is useful for the investigation of internal dimensions and shape, type, and properties of fill, void within the fill, cracks [71] and voids within the fabric of the structure, etc. of retaining walls, wing walls, spandrel walls, harbor deck wall, and road surface. The limitation of the method is that it is often difficult to distinguish reflections from surface wave and refracted arrivals [4, 9, 71].

3.1.4. Ultrasonic reflection method

Ultrasonic reflection methods are used for locating and identifying flaws in concrete and detecting small defects in the concrete wall. A piezoelectric transducer produces above 20 kHz ultrasonic waves that propagate 50 to 100 mm masonry. The method is less effective in higher attenuation characteristics concrete with many material boundaries which scatter both incident and reflected waves. The method is not commonly used for some difficulties such as lack of good coupling of the transducer to the surface, difficult to achieve adequate coupling with some of the uneven surface. The coupling agents such as grease or petroleum or temporary adherence limits the scattering of the signal through the materials and make the complexity of return noise. As a result, the observer might confuse surface wave with compression wave [9].

3.1.5. Sonic resonance method

This method helps to detect defects or cavities behind the linings of tunnels or areas of a rendered wall. A lightweight hammer is tapped on the line or rendered wall, and the reflective echo from the defects or cavities produce a notable change in the frequency of the wave.

2.9 Acoustic emission method

Acoustic method is a nondestructive method that surveys the existing civil engineering structures for detecting prestressed cable failure and cracks in concrete [72]. Fig. 24 shows the acoustic emission instrumentations. Acoustic emission method is deployed for bridge health monitoring by many researchers [73-78]. Yu et al. (2011) used acoustic emission method to predict fatigue crack in steel bridge [79]. This method is also used for monitoring damage initiation and propagation carbon fiber-reinforced-polymer (CFRP) stay cables in bridge [80, 81]. Colombo et al. (2003) developed 'b-value' analysis method for assessing reinforced concrete beam based on acoustic emission method [82].



Figure 24: Acoustic emission arrangement [83]

Applications of acoustic emission method are [84]

1. Continuous damage growth monitoring of concrete.
2. Fracture type, orientation, size, and energy determination.
3. Recording failure process of a structure under load condition.
4. Detecting rebar corrosion at early stage [85].
5. Assessment of the nature of process zone. Process zone is the region of discontinuous crack ahead of visible continuous crack [33].

The limitation of the acoustic emission is that the energy released by this method is smaller than the ultrasonic techniques signal. For this reason, more sensitive sensor, reliable amplifier, and pre-amplifier are required, and using these instruments creates problems such as the influence of ambient noise, attenuation of the signal and sometimes low signal to noise ratio. As a result, sophisticated instruments are needed to detect and localize the damage pattern [86].

2.10 Covermeter

Covermeter measures the concrete cover thickness over the reinforcement and locates the rebar location. Commercially available covermeter is Profoscope as shown in fig. 25. It detects rebar by electromagnetic pulse induction (as shown in fig. 26).

Applications of covermeter are:

1. Rebar location determination.
2. Rebar spacing determination.
3. Concrete cover determination.

4. Bar diameter estimation.
5. Mid-point between bars evaluation.
6. Bar orientation assessment.



Figure 25: Profoscope to detect rebar location [87, 88]

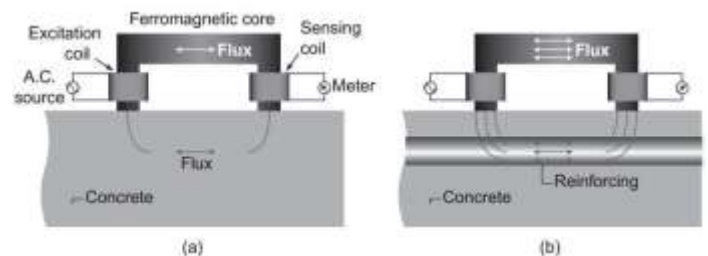


Figure 26: (a) sensing coil produces a small flux when the covermeter is placed on a nonreinforced area; (b) the sensing coil measure a high flux when reinforce is present in the concrete [33].

2.11 Maturity Method

The principal of maturity method is based on hydration of cement time and temperature. There are three different concrete maturity index estimation methods: Nurse-Saul (Temperature-Time factor), Arrhenius (Equivalent age), and Weighted maturity. The author only discussed Nurse-Saul method in this article. The Nurse-Saul method assumes that the initial rate of strength gain is a linear function of temperature.

A maturity function $M(t)$ consists of the time interval (Δt), average concrete temperature (T_a) and the datum temperature (T_0). A datum temperature of 0°C or 32°F is recommended by ASTM C 1074.

$$M(t) = \sum (T_a - T_0) \Delta t$$

The use of maturity monitoring is in-situ strength for post-tensioned decks, in-situ strength for form-jumping or cycling, and mass concrete protection or thermal cracking. Fig. 27 shows the concrete maturity meter.



Figure 27: Maturity meter SensorConcrete [89]

2.12 Stress wave propagation method

Deformation in a material caused by waves from impact between materials, explosions, and earthquakes etc. is called stress wave. Stress from static loads and dynamic loads has an enormous difference. The load application time for the static load is long while the load application time for the dynamic load is a few seconds with a magnitude higher than static loading. This makes the phenomena complex for analysis, and the materials behave differently than normal. A dangerous large deformation is created when the shock velocity is high, and it creates plastic and elastic deformation in the material.

Lei et al. (2017) used stress waves along a rock bolt to develop Automatic Extract Algorithm (AEA) method based on the self-correlation analysis and statistical analysis [90] as shown in fig. 30. A large pre-stress force is applied on the rock bolt to minimize the loose movement of the rock [91]. Piezoceramic transducers and Lead Zirconate Titanate (PZT) are used to detect the reflected stress wave and a giant magnetostrictive (GMS) transducer is used to generate the stress on the exposed end of the rock bolt [92]. The arrival time of the wave from the end of the rock bolt and the periodicity is then determined. From the interval time, the length of rock bolt is calculated. AEA is faster than traditional Phase Analysis Method (PAM).

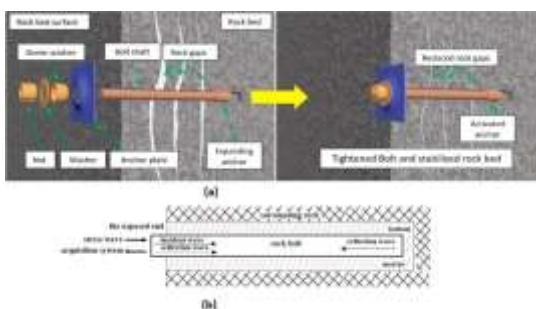


Figure 28: (a) Rock bolt reinforced rock masses; (b) schematic diagram of rock bolt mechanism [90]

2.13 Corrosion potential test

Corrosion initiation of reinforcement steel is caused by ingress of carbon dioxide and chloride ions to the steel surface [93]. After corrosion initiation, iron oxide and hydroxides are deposited in the restricted space of concrete around the steel. Their initiation creates expansive stress on concrete and makes concrete crack and spall the concrete cover. Corrosion maintenance needs a substantial portion of national budget. ASTM C 876 described the criteria for corrosion of steel. Rebar corrosion can be assessed by the following techniques [94]:

1. Embeddable corrosion monitoring sensor.
2. Cover thickness measurements.
3. Ultrasonic pulse velocity technique.
4. X-ray, Gamma radiography measurement.
5. Infrared thermograph Electrochemical.
6. Galvanostatic pulse transient method.
7. Electrochemical impedance spectroscopy (EIS).
8. Harmonic analysis.
9. Noise Analysis.
10. Open circuit potential (OCP) measurements.
11. Surface potential (SP) measurements.
12. Concrete resistivity measurement.
13. Linear polarization resistance (LPR) measurement.
14. Tafel extrapolation.
15. Visual inspection

Due to space restriction of the paper, the author of this paper discusses embeddable corrosion monitoring sensor, Vibrating wire and electrical strain gauges, Galvanostatic pulse transient method, and Linear polarization resistance (LPR) measurement. Ultrasonic pulse velocity technique, Infrared thermograph Electrochemical and Cover thickness measurements are discussed above. Electrochemical impedance spectroscopy (EIS) and X-ray, Gamma radiography measurement are discussed below.

2.13.1 Embeddable corrosion monitoring sensor

Early warning condition of crack, spall, and other deterioration of concrete steel can be provided by the Embedded Corrosion Instrument (ECI) sensor. ECI gives real-time, comprehensive information of structural condition by monitoring chloride ion concentration, temperature, linear polarization resistance, open circuit potential, and resistivity of concrete. The ECI-1 sensor as shown in fig. 31 incorporates

5 sensors rugged in a small package. It is easy to install and can place where adequate attention needed. Many authors discussed about remote monitoring of corrosion potential by ECI-1 sensor [95-100].

Advantages of ECI

1. The ECI has capability to monitor flood control channels, bridges, buildings, roadways, dams, spillways, erosion control structures, parking garages, piers, and pylons.
2. The ECI offers the opportunity to the inspectors to inspect the structure without cut the sample, interruption of using structure and even visit the site.
3. The ECI comprehensive data correlates among the causes and signs of corrosion and yield a certain picture of threat.



Figure 29: ECI-1 sensor during operation [101]

2.13.2 Vibrating wire and electrical strain gauges

Vibrating wire strain gauges exhibit good strain measuring capability caused by stress variations. If the elastic modulus of concrete is known, stress can also be evaluated from strain. Fig. 32 shows the vibrating wire stain gauge and fig. 33 shows the vibrating wire in rebar arrangement. Electrical strain gauges cannot be embedded in the concrete mix for crack and delamination detection and it requires bonding surfaces. Vibrating wire strain gauges for wireless health monitoring of structures are discussed in these articles [102-104].

Advantages of Vibrating wire gauges:

1. Long-term reliability for absolute strain measurement.
2. Capable of transmitting signal over a long distance.
3. Detect delamination and internal crack of concrete.



Figure 30: vibrating wire embedment strain gauge [105]



Figure 31: Vibrating wire gauges used in rebar to monitor strain [106]

2.13.3 Galvanostatic pulse transient method

The Galvanostatic Pulse Measurements technique (GPM) is used in GalvaPulse to determine the corrosion rate and amount of rebar is being dissolved per year. One end of the GalvaPulse relates to reinforcement to induce a short duration current pulse and other end together with reference electrode place on a concrete surface to serve as counter electrode as shown in fig. 34. By utilizing Stern Geary equation, the corrosion rate can be estimated. PISON workabout Pro3 software package give the corrosion rate and mapping parameters. Rebar corrosion rate monitoring by Galvanostatic pulse transit method are discussed by many authors [107-110].

Advantages of GalvaPulse:

1. Rebar corrosion estimate within less than 10 seconds.
2. In wet, inhibitor treated or carbonated concrete it provides a reliable corrosion rate estimation.
3. The system is rapid, lightweight and easy to operate the software.
4. On curved or uneven surface, it also gives accurate estimation.

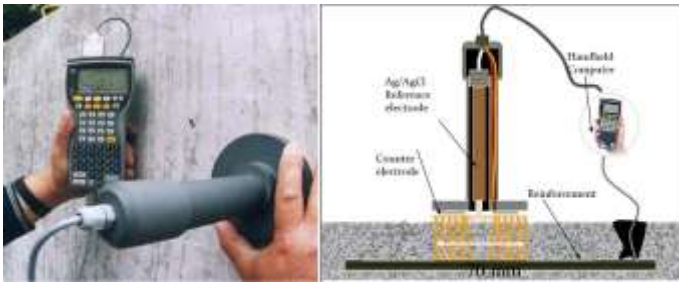


Figure 32: GalvaPulse and its working principle [111].

2.13.4 Linear polarization resistance (LPR) measurement

The LPR technique is a rapid, noninvasive method to estimate the instantaneous steel rebar corrosion rate [112]. Table-1 shows the typical corrosion rate. Fig. 32 shows the LPR instrumentation set up and its principle. The advantages of LPR are lightweight, instantaneous corrosion rate measurement, and straightforward data presentation and processing.

Table-1: Typical corrosion rates [113]

Corrosion Classification	Corrosion Current Density i_{corr}	Corrosion Penetration Rate
Passive/Very Low	Up to 0.2 $\mu\text{A}/\text{cm}^2$	Up to 2 $\mu\text{m}/\text{year}$
Low/Moderate	0.2 $\mu\text{A}/\text{cm}^2$ to 0.52 $\mu\text{A}/\text{cm}^2$	2 $\mu\text{m}/\text{year}$ to 6 $\mu\text{m}/\text{year}$
Moderate/High	0.5 $\mu\text{A}/\text{cm}^2$ to 1.06 $\mu\text{A}/\text{cm}^2$	6 $\mu\text{m}/\text{year}$ to 12 $\mu\text{m}/\text{year}$
Very High	> 1.0 $\mu\text{A}/\text{cm}^2$	> 12 $\mu\text{m}/\text{year}$

4. Time consuming, labor-oriented and expert personnel required.

5. The method requires smooth, uncoated, uncracked, and moisture-free concrete surface.

2.14 X-ray Computed tomography

Using projections of an object and X-ray, the image of an object can be reconstructed. An X-ray radiation source is rotated 360-degrees around the inspected object, and at the opposite side of the source, the detector measures the attenuation of the radiation penetrating through the material as shown in fig. 36. At the source-detector plane, computerized reconstruction algorithm reconstructs a cross-sectional image of the structure. There are two geometries: fan beam and parallel beam geometry. Parallel beam geometry has little practical use. Fan beam geometry is used in all medical scanners. Department of Civil and Environment Engineering, University of Washington is using NSI X5000 scanning system for 2D X-ray images, 3D computed tomography models and geometry and density digital information [115]. ASTM E2767 – 13 described the standard procedure for X-ray tomography.

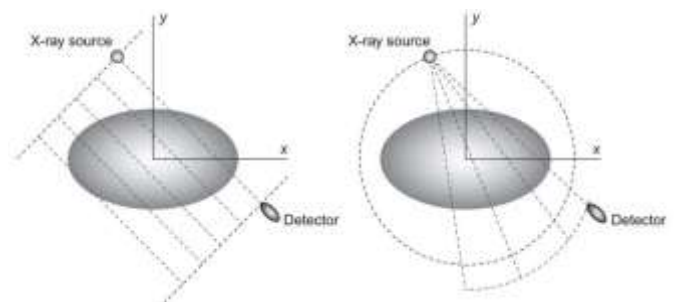


Figure 34: Parallel beam and fan-beam geometry [33]

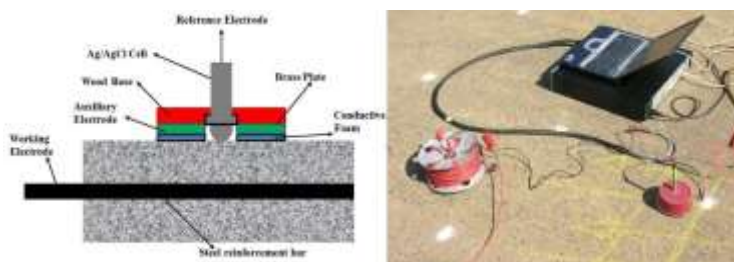


Figure 33: LPR schematic diagram (left) and instrument set up (right). [114]

Limitations of LPR:

1. LPR is semi-destructive method because it requires connection with embedded reinforcement.
2. The method is not applicable for epoxy-coated bar.
3. Interpreting of the test results is not standard.



Figure 35: NSI X5000 scanning system for X-ray tomography [116]

Applications of X-ray tomography are locating rebar, the existence of discontinuities, rebar corrosion, and presence of voids. However, the application of X-ray tomography is limited due to heavy and expensive equipment, high initial

cost, low speed, require highly skilled operators, safety precautions, both sides of structure assessment requirement [117]. The test results depend on the scattering of radiation into the off-beam detector, total photon count, the energy of radiation, and data sampling rate [33].

2.15 Electrical impedance spectroscopy (EIS)

EIS is a useful tool for corrosion research [118]. The methodology has been used to coatings, corrosion inhibitors, pitting corrosion, and polymer coating study. Gamry's EIS300 software uses Galvanostatic, Potentiostatic, Hybrid, and OptiEIS model to compute impedance spectra. Reference 3000 EIS instrument can measure critical pitting corrosion temperature, leakage rate, and impedance spectra. ISO 16773-1:2016 provides the standard guideline for EIS.



Figure 36: Reference 3000 Electrical impedance spectroscopy [119]

The EIS has limited field application for the following reasons [33]:

1. The equipment is bulky and complex. It needs a frequency analyzer, a signal generator, and a potentiostat.
2. The entire rebar needs polarization. The measurements provide average value along the rebar.
3. The method is time-consuming and semi-destructive because it needs physical condition with the embedded rebar.

2.16 Wireless Sensor Network (WSN)

The SHM systems through wireless sensor networks (WSN) provides an opportunity to repair, reduce the maintenance cost and retrofit of the structure through its lifetime. Traditional SHM approaches suffer from problems like expensive sensor installation/wiring, signal degradation along lengthy cables, and data flooding. With the rapid wireless technology systems, WSN offers low-cost instrumentation with fast and dense deployment and easier

maintenance of sensors. It increases the accuracy of the collected SHM data using their on-board computational and wireless communication capabilities [120]. Kiremidjian and Straser (1998) were the first who used wireless sensor for structural health monitoring to reduce the health monitoring cost [121].

Advantages of wireless sensor instrumented structures are [122]:

1. Evaluation of the behavior of structure in service condition.
2. Dynamic characteristics determination.
3. Structural performance monitoring at induced excitations.
4. Structural design security revision with previous regulation.
5. Detection of potential danger due to the damage in the structure.
6. Collected information can be used for hypothesis verification and results of diverse mathematic models (for example allows calibrating of finite element method).
7. Extrapolation of the actual response of the structure for expected a strong earthquake.
8. Facilitate the decision makers to make repair, maintenance or rehabilitation as a safeguard of the occupants.

Jerome P Lynch et al. performed a field validation test of wireless sensor on the Alamosa Canyon Bridge, located in Truth or Consequences, New Mexico, constructed in 1937. The 50ft long and 24ft wide bridge has 7in. concrete deck supported by six W30x116 steel girder. Two excitation inputs were considered to produce a sizable vibration response: the first one is impact blow on the span from a model hammer and the second excitation source was a large truck driven at 40 miles per hour over a wood plank placed at the center of the span instrumented as shown in fig. 29. Wireless sensors were installed upon the bridge girder and a commercial tethered monitoring system is installed parallel to the wireless sensor to permit a baseline for performance. Dactron SpectraBook dynamic signal analyzer was the data acquisition system with 8 simultaneous input channels and 21kHz sampling rate. Piezotronics PCB336C accelerometer used in cable-based monitoring system to measure dynamic response of the vridge and Crossbow CXL01LF1 MEMS accelerometer used in wireless sensing unit to measure bridge vibration. One of the channels of SpectraBook was directly connected to the accelerometer mounted on the structure. From the SpectraBook, a Window-based laptop with RT PRO Signal Analysis software control the system and collect data. A Linux-based laptop with a custom designed data acquisition system control and collect data from the wireless communication channel of the wireless sensing unit. To measure the input force from the model, hammer a load cell instrumented on the tip of the hammer. Impact point of

the hammer was the center of the deck (with respect to both length and width). Fig. 30 shows the accelerometer installation locations. All accelerometers were mounted at the midpoint of the girder's web except for Location S4. PCB336 accelerometer installed at the girder midpoint and CXL01LF1 with wireless sensing unit placed upon the girder flange. 7 tests were performed to measure acceleration at all sensor locations resulting 14 time-history recording (7 generated by Dactron System and 7 from wireless sensor unit). The Dactron systems employs RT Pro Signal Analysis to compute the frequency response function from time-history data. The embedded FFT algorithm (this implementation employs the Cooley-Turkey FFT algorithm) in wireless sensor unit calculated the frequency response function and transmitted to a laptop. From the frequency response function 6.7, 8.2 and 11.4 Hz response were evident. They concluded that the wireless sensor gives a good agreement with wired sensor data and the installation time for the wireless sensor is half of the time taken by wired sensors. There is a disagreement in the frequency response function at low frequency [123].



Figure 37: Model hammer excitation (left) and flatbed truck driving over a wood stud place on the center of the span (right) [123].

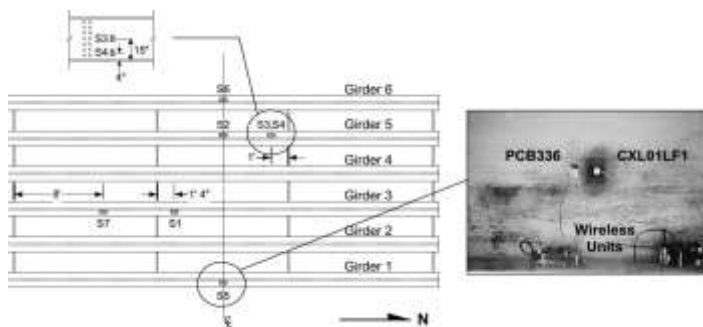


Figure 38: Accelerometer installation locations [123]

Academic and commercial wireless sensors platforms are proposed for SHM. Table 1 and

Table 2 gives a comprehensive summary of the performance features of the academic and commercial prototypes. Table 3 shows a comparison between wireless and wired sensors feature.

Table -2: Development of academic wireless sensor platform 1998 to 2009 [124-132]

Developer and Year	Processor	Radio	Frequency	Data Rate
Straser, Kiremidjian and Meng [128]	Motorola 68HC11	Proxim/ProxLink	900 MHz	19.2 kbps
Bennett et al. [129]	Hitachi H8/329	Radiometrix	418 MHz	40 kbps
Lynch [130]	Atmel AVR8515	Proxim RangeLan2	2.4 GHz	1.6 Mbps
Mitchell, Rao and Pottinger [131]	Cygnal 8051	Ericsson Bluetooth	2.4 GHz	--
Kottapalli et al. [132]	Microchip PIC16F73	BlueChip RBF915	900 MHz	10 kbps
J. Lynch et al. [133]	AV90S8515	Proxim RangeLan2	2.4 GHz	1.6 Mbps
Aoki, Fujino and Abe [134]	Renesas H8/4069F	RealtekRTL-8019AS	-	--
Basheer, Rao and Derriso [135]	ARM7TDMI	Philips Blueberry	2.4 GHz	--
Casciati et al. [136]	-	Aurel XTR-915	914.5 MHz	100 kbps
Wang et al. [137]	Analog ADuC832	Linx Technologies	916 MHz	33.6 kbps
Mastroleon et al. [138]	Microchip PIC-micro	BlueChip RFB915B	900 MHz	19.2 kbps
Sazonov, Janoyan and Jha [139]	MSP 430F1611	Chipcon CC2420	2.4 GHz	250 kbps
Farrar et al. [140]	Intel Pentium	MotorolanueRFon	2.4 GHz	230 kbps
Pei et al. [141]	Motorola 68HC11	Max-stream Xstream	2.4 GHz	Research
Musiani, Lin and Rosing [142]	ATMega128L	ChipconCC1100	1 MHz	0.6-250 kbps
Wang, Lynch and Law [143]	ATMega128	9XCite	900 MHz	26 kbps
Bocca et al. [144]	MSP430	ChipconCC2420	2.4 GHz	20 kbps
Zhou et al. [145]	MSP430	ChipconCC2500	2.4 GHz	250 kbps
Zhu et al. [146]	Atmega128	XStream	2.4 GHz	20 kbps

Table -3: Commercial sensing unit protocol [126]

Developer and Year	Processor	Radio	Frequency Brand	Data Rate
UC Berkeley Crossbow WeC (1999)	Atmel AT90LS8535	TR1000	868 / 916 MHz	10 kbps
UC Berkeley Crossbow Rene (2000)	Atmega163L	TR1000	868 / 916 MHz	10 kbps
UC Berkeley Crossbow MICA (2002)	ATmega103L	TR1000	868 / 916 MHz	40 kbps
UC Berkeley Crossbow MICA2 (2003)	ATmega128L	Chipcon CC1000	315, 433, or 868 / 916MHz	38.4 kbps
Intel iMote, Kling (2003)	Zeevo ARM7TDMI	Wireless BT Zeevo	2.4 GHz	600 kbps
Microstrain, Galbreath et al. (2003)	MicroChip PIC16F877	RF Monolithics DR-3000-1	916.5 MHz	75 kbps
Rockwell, Agre et al. (1999)	Intel StrongARM 1100	Conexant RDSSS9M	916 MHz	100 kbps

Table -4: Commercial sensing unit protocol [126]

Type	Cost	Flexibility	Design Level	Sensibility to environmental effect
Wireless sensor system for SHM	Economic (approx. \$100)	Yes	Difficult	Yes
Wired sensor system for SHM	Expensive (approx. \$1,000)	No	Easy	No

3. Summary Table

Table-5 shows the measurements, applications, advantages, limitation, instrumentation, and standards of all Nondestructive techniques as discussed above.

Table-5: Summary of all NDT techniques that are discussed above

NDT techniques	Measurement	Instruments	Standards	Application/Advantage	Limitation
Surface hardness method	Measure surface hardness of concrete	1.Schmidt OS-120 hammer 2. Silver Schmidt hammer	ASTM C 805	Inexpensive, quick and user-friendly hammer surface harness method	The result depends on the type and amount of aggregate, wet/dry surface, surface carbonation, location of plunger.
Penetration resistant method	From the depth of penetration, the device estimates the concrete strength	Windsor HP Probe system- 3 probes, equilateral triangle template, cartridge.	ASTM C 803	Though Windsor Probe test is costly compared to surface hammer test, it is superior to hammer test because it measures not only surface hardness but also concrete inside hardness. It is an excellent method for determining the stripping time for formworks.	The variation in data in Windsor Probe test is higher than surface hardness method. Repair of damage concrete is required.
Pullout Test	Shear strength of concrete from the force required to pull out of concrete.	1.Hydrajaws 2050 Deluxe 2. Hydrajaw Model 2000 Deluxe pull tester with Bluetooth technology	ASTM C 900	The test provides practical results for the optimum time of safe form-stripping, determining concrete strength for carrying out post-tensioning, evaluation of curing period based on target strength. As larger volume and greater depth of concrete are involved in this test, this test is superior than hammer and penetration test (Malhotra).	It does not provide statistical procedure to measure other strength properties. The steel rod must be embedded during the pouring of concrete and hence the test cannot be undertaken at later ages. As it pulls out a concrete portion, repair is required after the test.
Maturity Method	Concrete maturity	Maturity meter SensorConcrete	ASTM C 1074, C918, ACI 228.1R, 318, 306R, DOT specifications, NEN 5970	The use of maturity monitoring is: in-situ strength for post-tensioned decks, in-situ strength for form-jumping or cycling, and mass concrete protection or thermal cracking.	--
Stress wave propagation method	Length of rock bolt and development of automatic extraction algorithm (AEA)	Piezoceramic transducers, Lead Zirconate Titanate (PZT), and a giant magnetostrictive (GMS) transducer	--	AEA is faster than traditional Phase Analysis Method (PAM).	The method has few field validations. For more accuracy more field validation is required.
Ultrasonic pulse velocity method	concrete homogeneity, dynamic elastic modulus, voids, honey combs, cracks and other non-homogeneous condition, concrete strength	Ultrasonic pulse velocity tester (58-E4800 UPV tester)	ASTM C 597 IS 13311 (Part 1):1992 BS 1881: Part 203: 1986 BS 4408: Part 5 BS 12504-4, Part 4 2004	1.Evaluation of concrete homogeneity and dynamic elastic modulus. 2.Inspection of prestressed and precast beams, new and old structure, fire damaged areas, columns, slabs, concrete forms and other structures. 3.Detection of voids, honey combs, cracks and other non-homogeneous condition of the concrete. 4.PULSONIC model 58-E4900 combined with oscilloscope can do Spectrum analysis by FFT method, evaluation of	1.If the factors data as discussed above are not available, assessment of concrete compressive strength by UPV provides 95% confidence level which is 15 to 20% depends on concrete mix design data available. 2.For better result of new and old structure, the methods need the incorporation of concrete hammer methods.

Impact-echo method	Honeycombing, voids, wall thickness, metal and concrete bonds, and flaws inside the plate-type structure.	spherical impactors, analog to digital data acquisition systems, a hand-held transducer unit, a computer, and a software package	ASTM C 1383	Impact-echo method is successfully used to detect: 1. Basement wall and marine spun piles honeycombing. 2. Prestressed beams and slabs tendon ducts voids. 3. Retaining wall thickness. 4. Metal and concrete bonds in railways ties. 5. Flaws inside the plate-type structure such as garage slabs, plaza deck slabs and foundation walls.	--
Acoustic emission method	Fracture type, orientation, size and energy determination, rebar corrosion at early stage, and continuous damage growth monitoring of concrete.	Pocket AE-1 consists of single-channel AE unit, 1m sensor cable, a battery eliminator DC power supply	--	1. Continuous damage growth monitoring of concrete. 2. Fracture type, orientation, size and energy determination. 3. Recording failure process of a structure under load condition. 4. Detecting rebar corrosion at early stage [85]. 5. Assessment of the nature of process zone. Process zone is the region of discontinuous crack ahead of visible continuous crack [33].	1. Energy released by this method is smaller than the ultrasonic techniques signal. 2. More sensitive sensor, reliable amplifier and pre-amplifier are required.
Covermeter	Rebar location, spacing, concrete cover, bar diameter, and bar orientation	Profoscope	ACI 228.2R-98	1. Rebar location determination. 2. Rebar spacing determination. 3. Concrete cover determination. 4. Bar diameter estimation. 5. Mid-point between bars evaluation. 6. Bar orientation assessment.	
Ground penetration radar	Detect voids and delamination's, rebar location and arrangement, material interface changes and pavement thickness	Leica DS2000 4 Wheel Radar Utility Detector	ASTM D6087-08 ASTM D6432-11	1. Rapid, reliable, repeatable, and well-established data acquisition method. 2. Well correlated between corrosive environment and electrical resistivity. 3. The method is popular to detect voids and delamination's, rebar location and arrangement, material interface changes and pavement thickness.	1. Expert people need to data acquisition, processing and interpretation. 2. It is costly when applied for an individual structure. 3. Signal penetration is attenuated when de-icing agent is used on the structure. 4. In extremely cold condition there is negative data. 5. Within the upper half of the deck, GPR can easily identify the corrosive rebar but for lower half it is difficult to detect due to upper half rebar mat. 6. Deck delamination cannot assess directly by GPR. 7. GPR signal attenuated due to conductive soil, wet clay, salt water saturated water, etc.

Infrared thermography	Cannel seepage, moisture detection, source of stress location, deeper voids, crack detection, water pipe leakage detection.	InGaAs SWIR Camera: A6200sc	ASTM C1060 (envelope cavities of frame buildings), ASTM C1153 (wet insulation in roofing systems), ATSM D4788 (delamination in bridge decks), ASTM E1186 (air leakage site detection in building), ASTM E1934 (examining electrical and mechanical equipment)	Remote sensing, large monitoring capacity, visibility, range of measurement, data manipulation, portability, and fast response rate. Cannel seepage identification, moisture detection on the surface, finding the source of stress location, deeper voids, crack detection as well as qualitative and quantitative applications in cultural heritage and civil engineering structures, buried water pipe leakage detection, detect heat losses, missing or damaged thermal insulation in walls and roofs, thermal bridges, air leakage and moisture sources in building.	--
Corrosion potential test	Corrosion rate of rebar	ECI-1 sensor, GalvaPulse	ASTM C 876	1. ECI-1 offers the opportunity to the inspectors to inspect the structure without cut the sample, interruption of using structure and even visit the site. 2. GalvaPulse provides rebar	1. LPR is semi-destructive method because it requires connection with embedded reinforcement, it is time consuming, labor orientated, and the test is not standard.
X-ray tomography	Reconstruction of object 2D image, 3D computed tomography models and geometry and density digital information	NSI X5000 scanning system	ASTM E2767 - 13	Locating rebar, existence of discontinuities, rebar corrosion, presence of voids, 2D X-ray images, 3D computed tomography models and geometry and density digital information	Heavy and expensive equipment, high initial cost, low speed, require highly skilled operators, safety precautions, both sides of structure assessment requirement
Electrical impedance spectroscopy (EIS)	Coatings, corrosion inhibitors, pitting corrosion, and polymer coating study	Reference 3000	ISO 16773-1:2016	Coatings, corrosion inhibitors, pitting corrosion, and polymer coating study	Bulky and complex equipment, semi-destructive, time consuming, and labor-oriented.
Wireless sensor network	Dynamic characteristics, structural performance, structural design security revision.	Shown in Table-2	--	Evaluation of the behavior of structure, dynamic characteristics, structural performance, structural design security revision, detection of potential danger, hypothesis verification and results of diverse mathematic models, extrapolation of the actual response of the structure for expected a strong earthquake, facilitate the decision makers to make repair, maintenance or rehabilitation.	Difficult to design and it is sensitive to the environmental effect.

4. CONCLUSION

It is important to maintain a safe and reliable structural health condition. Different non-destructive tools are needed for assessing the integrity of structure and the nature of the damage. To achieve this, the inspectors need to know the types of tools and their suitability for different purposes which have been carried out in structural health monitoring field in the past. The author analyzes a comprehensive list of non-destructive tools, and their applications, standard code, latest equipment's, advantages, and limitations.

1. Ultrasonic pulse velocity, impact echo, impulse radar, and conductivity test are recommended for bridge evaluation.
2. For effective evaluation of stone masonry structures, ultrasonic pulse velocity method, acoustic-based method, and radar method are best suitable [133].
3. Radar methods and penetrating radiation methods are recommended for brick masonry structures.
4. Among the many corrosion techniques, the linear polarization method is most recommended for RCC structures.
5. Ground penetration method, infrared thermography, impulse echo method and ultrasonic pulse velocity methods are recommended for voids, cracks, honey-combing and non-homogeneity detection of concrete.
6. Pullout test is the best tool for evaluation of safe form stripping of concrete for a certain targeted strength.
7. Infrared thermography method is the best tools for condition assessment of all structures.

5. REFERENCES

- [1] Khawwam. (2004). International workshop on preservation of historical structures with FRP composites. Available: <https://www.slideshare.net/Khawwam/8-tests-for-concrete>
- [2] E. Sheils, A. O'Connor, F. Schoefs, and D. Breyse, "Investigation of the effect of the quality of inspection techniques on the optimal inspection interval for structures," *Structure and Infrastructure Engineering*, vol. 8, no. 6, pp. 557-568, 2012.
- [3] D. Breyse, G. Klysz, X. Dérobert, C. Sirieix, and J. Lataste, "How to combine several non-destructive techniques for a better assessment of concrete structures," *Cement and Concrete Research*, vol. 38, no. 6, pp. 783-793, 2008.
- [4] "Federal Highway Administration Research and Technology Nondestructive Evaluation (NDE) GPR Web Manual," ed, 2017.
- [5] D. Breyse and O. Abraham, "Guide méthodologique de l'évaluation non destructive des ouvrages en béton armé," Presses ENPC, Paris, 2005.
- [6] J. Bungey, S. Millard, and M. Grantham, "Ultrasonic pulse velocity methods," *Testing of Concrete in Structures*, Taylor & Francis, New York, 2006.
- [7] T. Uomoto, *Non-destructive testing in civil engineering 2000*. Elsevier, 2000.
- [8] P. Das and M. Hardy, "Specifications for competitive tendering of NDT inspection of bridges," in *BRIDGE MANAGEMENT 4-INSPECTION, MAINTENANCE, ASSESSMENT AND REPAIR*, 2000.
- [9] D. McCann and M. Forde, "Review of NDT methods in the assessment of concrete and masonry structures," *Ndt & E International*, vol. 34, no. 2, pp. 71-84, 2001.
- [10] V. Malhotra and V. Sivasundaram, "Resonant Frequency Methods. In.: MALHOTRA, VM; CARINO, NJ (Eds.). Handbook on Nondestructive Testing of Concrete. West Conshohocken," ed: CRC Press LLC (ASTM International), 2004.
- [11] A. Monteiro and A. Gonçalves, "Assessment of characteristic compressive strength in structures by the rebound hammer test according to EN 13791: 2007," ed: NDTCE.
- [12] "NDT Bridges," 2017.
- [13] (2017). Ultrasonic pulse velocity tester, Concrete testing equipment, Controls. Available: <http://www.controls-group.com/eng/concrete-testing-equipment/ultrasonic-pulse-velocity-tester.php>
- [14] B. S. Al-Nu'man, B. R. Aziz, S. A. Abdulla, and S. E. Khaleel, "Effect of Aggregate Content on the Concrete Compressive Strength-Ultrasonic Pulse Velocity Relationship," *American Journal of Civil Engineering and Architecture*, vol. 4, no. 1, pp. 1-5, 2016.
- [15] Designed and w. m. c. Promoted by Maharashtra Industries Directory, "Ultrasonic Pulse Velocity Test, Ultrasonic Pulse Velocity Testing Instruments, Pune, India," ed, 2017.
- [16] A. Samarin and P. Meynink, "Use of combined ultrasonic and rebound hammer method for determining strength of concrete structural members," *Concrete International*, vol. 3, no. 03, pp. 25-29, 1981.
- [17] I. Facaoaru, "Contribution a l'étude de la relation entre la résistance du béton a la compression et de

- la vitesse de propagation longitudinale des ultrasons," RILEM Bull, vol. 12, pp. 125-154, 1961.
- [18] R. Hamid, K. Yusof, and M. F. M. Zain, "A combined ultrasound method applied to high performance concrete with silica fume," *Construction and Building Materials*, vol. 24, no. 1, pp. 94-98, 2010.
- [19] M. Machado, L. Shehata, and I. Shehata, "Correlation curves to characterize concretes used in Rio de Janeiro by means of non destructive tests," *Revista IBRACON de Estruturas e Materiais*, vol. 2, no. 2, pp. 100-123, 2009.
- [20] M. D. Machado, L. D. Shehata, and I. A. E. M. Shehata, "Curvas de correlação para caracterizar concretos usados no Rio de Janeiro por meio de ensaios não destrutivos," *RIEM-IBRACON Structures and Materials Journal*, vol. 2, no. 2, 2009.
- [21] E. Proverbio, V. Venturi, and S. Messina, "Reliability of nondestructive tests for on site concrete strength assessment," *10DBMC*, Lyon, France, 2005.
- [22] H. Y. Qasrawi, "Concrete strength by combined nondestructive methods simply and reliably predicted," *Cement and concrete research*, vol. 30, no. 5, pp. 739-746, 2000.
- [23] V. Sturup, F. Vecchio, and H. Caratin, "Pulse velocity as a measure of concrete compressive strength," *Special Publication*, vol. 82, pp. 201-228, 1984.
- [24] G. Trtnik, F. Kavčič, and G. Turk, "Prediction of concrete strength using ultrasonic pulse velocity and artificial neural networks," *Ultrasonics*, vol. 49, no. 1, pp. 53-60, 2009.
- [25] Ö. Ariöz et al., "Use of Combined Non-Destructive Methods to Assess the Strength of Concrete in Structures," 2009.
- [26] K. B. Najim and M. R. Hall, "Mechanical and dynamic properties of self-compacting crumb rubber modified concrete," *Construction and building materials*, vol. 27, no. 1, pp. 521-530, 2012.
- [27] D. Breyse, "Nondestructive evaluation of concrete strength: An historical review and a new perspective by combining NDT methods," *Construction and Building Materials*, vol. 33, pp. 139-163, 2012.
- [28] J. H. Bungey, "The testing of concrete in structures / J.H. Bungey - Details," 1989.
- [29] "SAMHITHA INNOVATIONS," ed, 2017.
- [30] "Concrete test hammer - Original Schmidt - Proceq - Videos," ed, 2017.
- [31] (2017). ASTM C805 / C805M - 13a Standard Test Method for Rebound Number of Hardened Concrete. Available: <https://www.astm.org/Standards/C805.htm>
- [32] A. Castañeda, F. Corvo, J. Howland, R. Marrero, and D. Fernández, "ATMOSPHERIC CORROSION OF STEEL-REINFORCED CONCRETE IN A COASTAL CITY LOCATED ON A TROPICAL ISLAND," *REINFORCED CONCRETE*, p. 109.
- [33] P. K. Mehta, "Concrete. Structure, properties and materials," 1986.
- [34] (2017). ASTM C803 / C803M - 17 Standard Test Method for Penetration Resistance of Hardened Concrete. Available: <https://www.astm.org/Standards/C803.htm>
- [35] "James Instruments," ed, 2017.
- [36] Khawwam, "8 tests for concrete," ed, 2017.
- [37] "Engineersdaily | Free engineering database: Penetration Resistance Test (ASTM C 803)," ed, 2017.
- [38] (2017). ASTM C900 - 15 Standard Test Method for Pullout Strength of Hardened Concrete. Available: <https://www.astm.org/Standards/C900.htm>
- [39] V. M. Malhotra, "Nondestructive tests," in *Significance of Tests and Properties of Concrete and Concrete-Making Materials: ASTM International*, 2006.
- [40] "Hydrajaws Model 2000 Digital Bluetooth System Anchor Pull Tester," ed, 2017.
- [41] "Engineersdaily | Free engineering database: Pull Out Test of Concrete," ed, 2017.
- [42] Gharpedia, "In-Situ Concrete Pull Out Test for Compressive Strength," ed: @gharpedia, 2017.
- [43] J. Martin, M. S. Hardy, A. S. Usmani, and M. C. Forde, "Accuracy of NDE in bridge assessment," *Engineering structures*, vol. 20, no. 11, pp. 979-984, 1998.
- [44] A. G. Davis, C. Dunn, and CEBTP, "From theory to field experience with the non-destructive vibration testing of piles," *Proceedings of the Institution of Civil Engineers*, vol. 57, no. 4, pp. 571-593, 1974.
- [45] N. J. Carino, M. Sansalone, and N. N. Hsu, "A point source-point receiver, pulse-echo technique for flaw detection in concrete," in *Journal Proceedings*, 1986, vol. 83, no. 2, pp. 199-208.

- [46] C. Cheng and M. Sansalone, "The impact-echo response of concrete plates containing delaminations: numerical, experimental and field studies," *Materials and Structures*, vol. 26, no. 5, pp. 274-285, 1993.
- [47] M. J. Sansalone and W. B. Streett, "Impact-echo. Nondestructive evaluation of concrete and masonry," 1997.
- [48] J. R. Peter Shaw, Torben Klitt Petersen, Christian Bernstone. (2004). A Practical Guide to Non Destructive Examination of Concrete. Available: https://www.researchgate.net/publication/305209558_A_Practical_Guide_to_Non_Destructive_Examination_of_Concrete
- [49] "IEI Products Page," ed, 2017.
- [50] J. Grove, K. Jones, D. Ye, and J. Gudimetta, "Nondestructive Tests of Thickness Measurements for Concrete Pavements: Tests Really Work," *Transportation Research Record: Journal of the Transportation Research Board*, no. 2268, pp. 61-67, 2012.
- [51] F. Khan, M. Bolhassani, A. Koutsos, A. Hamid, and I. Bartoli, "Modeling and experimental implementation of infrared thermography on concrete masonry structures," *Infrared Physics & Technology*, vol. 69, pp. 228-237, 2015.
- [52] "InGaAs SWIR Camera A6200sc," ed: PhotonicsOnline, 2017.
- [53] (2017). Infrared Thermography - An Overview | Calgary Home Inspection Services. Available: <https://www.assuredhi.com/infrared-thermography-overview/>
- [54] M. Clark, D. McCann, and M. Forde, "Application of infrared thermography to the non-destructive testing of concrete and masonry bridges," *Ndt & E International*, vol. 36, no. 4, pp. 265-275, 2003.
- [55] P. Engelbert, R. Hotchkiss, and W. Kelly, "Integrated remote sensing and geophysical techniques for locating canal seepage in Nebraska," *Journal of Applied Geophysics*, vol. 38, no. 2, pp. 143-154, 1997.
- [56] H. Wiggerhauser, "Active IR-applications in civil engineering," *Infrared Physics & Technology*, vol. 43, no. 3, pp. 233-238, 2002.
- [57] D. P. Rao, "Infrared thermography and its applications in civil engineering," *The Indian Concrete Journal*, vol. 82, no. 5, pp. 41-50, 2008.
- [58] R. W. Arndt, "Square pulse thermography in frequency domain as adaptation of pulsed phase thermography for qualitative and quantitative applications in cultural heritage and civil engineering," *Infrared Physics & Technology*, vol. 53, no. 4, pp. 246-253, 2010.
- [59] G. J. Weil, "Non contact, remote sensing of buried water pipeline leaks using infrared thermography," 1993: ASCE.
- [60] C. Balaras and A. Argiriou, "Infrared thermography for building diagnostics," *Energy and buildings*, vol. 34, no. 2, pp. 171-183, 2002.
- [61] A. Kylili, P. A. Fokaides, P. Christou, and S. A. Kalogirou, "Infrared thermography (IRT) applications for building diagnostics: A review," *Applied Energy*, vol. 134, pp. 531-549, 2014.
- [62] P. A. Fokaides and S. A. Kalogirou, "Application of infrared thermography for the determination of the overall heat transfer coefficient (U-Value) in building envelopes," *Applied Energy*, vol. 88, no. 12, pp. 4358-4365, 2011.
- [63] S. Bagavathiappan, B. Lahiri, T. Saravanan, J. Philip, and T. Jayakumar, "Infrared thermography for condition monitoring—a review," *Infrared Physics & Technology*, vol. 60, pp. 35-55, 2013.
- [64] D. Cardone, M. Dolce, F. C. Ponzo, and E. Coelho, "Experimental behaviour of R/C frames retrofitted with dissipating and re-centring braces," *Journal of Earthquake Engineering*, vol. 8, no. 03, pp. 361-396, 2004.
- [65] F. Bisegna, D. Ambrosini, D. Paoletti, S. Sfarra, and F. Gugliermetti, "A qualitative method for combining thermal imprints to emerging weak points of ancient wall structures by passive infrared thermography—A case study," *Journal of Cultural Heritage*, vol. 15, no. 2, pp. 199-202, 2014.
- [66] G. Washer, R. Fenwick, N. Bolleni, and J. Harper, "Effects of environmental variables on infrared imaging of subsurface features of concrete bridges," *Transportation Research Record: Journal of the Transportation Research Board*, no. 2108, pp. 107-114, 2009.
- [67] "Tunnel & Wall Inspection," ed, 2017.
- [68] (2017). ASTM D6087 - 08 Standard Test Method for Evaluating Asphalt-Covered Concrete Bridge Decks Using Ground Penetrating Radar. Available: <https://www.astm.org/DATABASE.CART/HISTORICAL/D6087-08.htm>






- [69] "Challenges in Corrosion Mapping with GPR | FPrimeC Solutions," ed, 2016.
- [70] C. Colla, P. Das, D. McCann, and M. Forde, "Sonic, electromagnetic and impulse radar investigation of stone masonry bridges," *Ndt & E International*, vol. 30, no. 4, pp. 249-254, 1997.
- [71] P. McDowell et al., "Geophysics in engineering investigations," 2002.
- [72] R. Laloux and J. Robert, "ACOUSTIC EMISSION TECHNIQUES APPLIED TO CIVIL ENGINEERING STRUCTURES," 1986.
- [73] K. M. Holford and R. J. Lark, "Acoustic Emission Testing Bridges," 2005.
- [74] A. Nair and C. Cai, "Acoustic emission monitoring of bridges: Review and case studies," *Engineering structures*, vol. 32, no. 6, pp. 1704-1714, 2010.
- [75] L. Golaski, P. Gebiski, and K. Ono, "Diagnostics of reinforced concrete bridges by acoustic emission," *Journal of acoustic emission*, vol. 20, no. 2002, pp. 83-89, 2002.
- [76] Z. Gong, E. Nyborg, and G. Oommen, "Acoustic emission monitoring of steel railroad bridges," *Materials evaluation*, vol. 50, no. 7, 1992.
- [77] K. M. Holford, A. Davies, R. Pullin, and D. Carter, "Damage location in steel bridges by acoustic emission," *Journal of intelligent material systems and structures*, vol. 12, no. 8, pp. 567-576, 2001.
- [78] A. Ghorbanpoor and A. T. Rentmeester, "NDE of steel bridges by acoustic emission," in *Structural Engineering in Natural Hazards Mitigation*, 1993, pp. 1008-1013: ASCE.
- [79] J. Yu, P. Ziehl, B. Zárate, and J. Caicedo, "Prediction of fatigue crack growth in steel bridge components using acoustic emission," *Journal of Constructional Steel Research*, vol. 67, no. 8, pp. 1254-1260, 2011.
- [80] P. Rizzo and F. L. di Scalea, "Acoustic emission monitoring of carbon-fiber-reinforced-polymer bridge stay cables in large-scale testing," *Experimental mechanics*, vol. 41, no. 3, pp. 282-290, 2001.
- [81] S. Yuyama, K. Yokoyama, K. Niitani, M. Ohtsu, and T. Uomoto, "Detection and evaluation of failures in high-strength tendon of prestressed concrete bridges by acoustic emission," *Construction and building materials*, vol. 21, no. 3, pp. 491-500, 2007.
- [82] I. S. Colombo, I. Main, and M. Forde, "Assessing damage of reinforced concrete beam using "b-value" analysis of acoustic emission signals," *Journal of materials in civil engineering*, vol. 15, no. 3, pp. 280-286, 2003.
- [83] "Physical Acoustics AE Technology - Overview of Acoustic Emission NDT Technology," ed, 2017.
- [84] C. U. Grosse, H. W. Reinhardt, and F. Finck, "Signal-based acoustic emission techniques in civil engineering," *Journal of materials in civil engineering*, vol. 15, no. 3, pp. 274-279, 2003.
- [85] A. K. Farid Uddin, M. Ohtsu, K. M. Hossain, and M. Lachemi, "Simulation of reinforcement-corrosion-induced crack propagation in concrete by acoustic emission technique and boundary element method analysis," *Canadian Journal of Civil Engineering*, vol. 34, no. 10, pp. 1197-1207, 2007.
- [86] C. U. Grosse and M. Ohtsu, *Acoustic emission testing*. Springer Science & Business Media, 2008.
- [87] "Metal rebar locator - max. 180 mm | Profoscope - Proceq - Videos," ed, 2017.
- [88] Administrator. (2017). ratioTEC Prüfsysteme GmbH - Profoscope. Available: <http://www.ratiotec.com/en/85-me-und-prfgerte/bauinstandsetzung/459-profoscope>
- [89] "Maturity method Techniconcrete," ed, 2017.
- [90] M. Lei, W. Li, M. Luo, and G. Song, "An automatic extraction algorithm for measurement of installed rock bolt length based on stress wave reflection," *Measurement*, 2017.
- [91] S. C. M. Ho, W. Li, B. Wang, and G. Song, "A load measuring anchor plate for rock bolt using fiber optic sensor," *Smart Materials and Structures*, vol. 26, no. 5, p. 057003, 2017.
- [92] M. Luo, W. Li, B. Wang, Q. Fu, and G. Song, "Measurement of the Length of Installed Rock Bolt Based on Stress Wave Reflection by Using a Giant Magnetostrictive (GMS) Actuator and a PZT Sensor," *Sensors*, vol. 17, no. 3, p. 444, 2017.
- [93] A. Bentur, N. Berke, and S. Diamond, *Steel corrosion in concrete: fundamentals and civil engineering practice*. CRC Press, 1997.
- [94] H.-W. Song and V. Saraswathy, "Corrosion monitoring of reinforced concrete structures-A," *Int. J. Electrochem. Sci*, vol. 2, pp. 1-28, 2007.
- [95] K. Perveen, G. E. Bridges, S. Bhadra, and D. J. Thomson, "Corrosion potential sensor for remote monitoring of civil structure based on printed circuit board sensor," *IEEE transactions on instrumentation and measurement*, vol. 63, no. 10, pp. 2422-2431, 2014.

- [96] M. M. Andringa, J. M. Puryear, D. P. Neikirk, and S. L. Wood, "Low-cost wireless corrosion and conductivity sensors," in Proceedings of SPIE, 2006, vol. 6174, no. 1, pp. 61740X-61740X.
- [97] A. Mufti, "Integration of sensing in civil structures: development of the new discipline of civionics," Structural Health Monitoring and Intelligent Infrastructure, vol. 1, pp. 119-129, 2003.
- [98] M. M. Andringa, J. M. Puryear, D. P. Neikirk, and S. L. Wood, "In situ measurement of conductivity and temperature during concrete curing using passive wireless sensors," in Proc. SPIE Int. Soc. Opt. Eng., 2007, vol. 6529, no. 2, pp. 65293M/65291-65293M/65210.
- [99] Y. Chen, S. Munukutla, P. Pasupathy, D. P. Neikirk, and S. L. Wood, "Magneto-inductive waveguide as a passive wireless sensor net for structural health monitoring," in Proc. SPIE, 2010, vol. 7647, p. 764749.
- [100] M. M. Andringa, D. P. Neikirk, N. P. Dickerson, and S. L. Wood, "Unpowered wireless corrosion sensor for steel reinforced concrete," in Sensors, 2005 IEEE, 2005, p. 4 pp.: IEEE.
- [101] A. Agrawal et al., "Remote corrosion monitoring systems for highway bridges," Practice Periodical on Structural Design and Construction, vol. 14, no. 4, pp. 152-158, 2009.
- [102] S. Neild, M. Williams, and P. McFadden, "Development of a vibrating wire strain gauge for measuring small strains in concrete beams," Strain, vol. 41, no. 1, pp. 3-9, 2005.
- [103] H. Lee, J. Kim, K. Sho, and H. Park, "A wireless vibrating wire sensor node for continuous structural health monitoring," Smart Materials and Structures, vol. 19, no. 5, p. 055004, 2010.
- [104] B. Benmokrane, M. Chekired, and H. Xu, "Monitoring behavior of grouted anchors using vibrating-wire gauges," Journal of Geotechnical Engineering, vol. 121, no. 6, pp. 466-475, 1995.
- [105] "Vibrating Wire Embedment Strain Gauge - Soil Instruments," ed, 2017.
- [106] "Vibrating Wire Strain Gauges - Sisgeo," ed, 2017.
- [107] S. Sathiyarayanan, P. Natarajan, K. Saravanan, S. Srinivasan, and G. Venkatachari, "Corrosion monitoring of steel in concrete by galvanostatic pulse technique," Cement and concrete composites, vol. 28, no. 7, pp. 630-637, 2006.
- [108] J. González, A. Cobo, M. González, and S. Feliu, "On-site determination of corrosion rate in reinforced concrete structures by use of galvanostatic pulses," Corrosion Science, vol. 43, no. 4, pp. 611-625, 2001.
- [109] C. Lu and Y. Peiyu, "An algorithm of galvanostatic pulse method to determine the corrosion status of reinforcement in concrete," Corrosion science, vol. 42, no. 4, pp. 675-686, 2000.
- [110] B. Elsener, O. Klinghoffer, T. Frolund, E. Rislund, Y. Schiegg, and H. Böhni, "Assessment of reinforcement corrosion by means of galvanostatic pulse technique," in Proceedings of International Conference on Repair of Concrete Structures-From Theory to Practice in a Marine Environment, 1997, pp. 391-400.
- [111] "Half Cell Potential | Corrosion Test and CorroMap | PCTE," ed, 2017.
- [112] S. Millard and J. Broomfield, "Current Practice Sheet 132: Measuring the corrosion rate of reinforced concrete using linear polarisation resistance," Concrete-Crowthorne, vol. 37, no. 3, pp. 36-38, 2003.
- [113] C. Andrade and C. Alonso, "Corrosion rate monitoring in the laboratory and on-site," Construction and Building Materials, vol. 10, no. 5, pp. 315-328, 1996.
- [114] "Federal Highway Administration Research and Technology Nondestructive Evaluation (NDE)," ed, 2017.
- [115] (2017). X-ray Computed Tomography Facility | UW Civil & Environmental Engineering. Available: <https://www.ce.washington.edu/research/facilities/xray>
- [116] "X5000 | North Star Imaging," ed, 2017.
- [117] O. Büyüköztürk, "Imaging of concrete structures," Ndt & E International, vol. 31, no. 4, pp. 233-243, 1998.
- [118] F. Mansfeld, "Electrochemical impedance spectroscopy (EIS) as a new tool for investigating methods of corrosion protection," Electrochimica Acta, vol. 35, no. 10, pp. 1533-1544, 1990.
- [119] Gamry_Inst, "Testing Electrochemical Capacitors: Electrochemical Impedance Spectroscopy," ed: @Gamry_Inst, 2014.
- [120] C. Liu, J. Teng, and N. Wu, "A wireless strain sensor network for structural health monitoring," Shock and Vibration, vol. 2015, 2015.

- [121] A. Kiremidjian and E. Straser, "A modular wireless damage monitoring system for structures," ed: Report TR128, Blume Centre, Stanford CA, 1998.
- [122] M. Ruiz-Sandoval, X. Argueta, and R. Marcelin, "DYNAMIC CHARACTERIZATION OF BUILDINGS USING WIRELESS SENSOR NETWORKS."
- [123] J. P. Lynch et al., "Field validation of a wireless structural monitoring system on the Alamosa Canyon Bridge," in Smart structures and materials, 2003, pp. 267-278: International Society for Optics and Photonics.
- [124] B. Aygün and V. Cagri Gungor, "Wireless sensor networks for structure health monitoring: recent advances and future research directions," Sensor Review, vol. 31, no. 3, pp. 261-276, 2011.
- [125] S. Cho, C.-B. Yun, J. P. Lynch, A. T. Zimmerman, B. F. Spencer Jr, and T. Nagayama, "Smart wireless sensor technology for structural health monitoring of civil structures," Steel Structures, vol. 8, no. 4, pp. 267-275, 2008.
- [126] J. P. Lynch and K. J. Loh, "A summary review of wireless sensors and sensor networks for structural health monitoring," Shock and Vibration Digest, vol. 38, no. 2, pp. 91-130, 2006.
- [127] S. Yang, "Health monitoring of pavement systems using smart sensing technologies," Iowa State University, 2014.
- [128] M. Al Qurishee and I. Fomunung, "Smart Materials in Smart Structural Systems."
- [129] M. Al Qurishee, "Application of Geosynthetics in Pavement Design," 2017.
- [130] W. Wu, M. A. Qurishee, J. Owino, I. Fomunung, M. Onyango, and B. Atolagbe, "Coupling Deep Learning and UAV for Infrastructure Condition Assessment Automation," in 2018 IEEE International Smart Cities Conference (ISC2), 2018, pp. 1-7: IEEE.
- [131] M. Qurishee, I. Iqbal, M. Islam, and M. Islam, "Use of slag as coarse aggregate and its effect on mechanical properties of concrete," in International Conference on Advances in Civil Engineering, CUET, 2016, vol. 3, pp. 475-479.
- [132] M. A. Qurishee, "Low-cost deep learning UAV and Raspberry Pi solution to real time pavement condition assessment," 2019.

- [133] A. Hussain and S. Akhtar, "Review of Non-Destructive Tests for Evaluation of Historic Masonry and Concrete Structures," Arabian Journal for Science and Engineering, vol. 42, no. 3, pp. 925-940, 2017.

BIOGRAPHIES

- [1]  I have a diverse knowledge of fiber optics, drone, network engineering, construction management, and ITS. Passionate to learn new technology and new areas of knowledge.
- [2]  Five+ years hands-on extensive experience on linear and nonlinear finite element analysis (FEA,FEM).
- [3]  Babatunde Atolagbe is a transportation engineer in the bridge inspection and remedial engineering unit at the Maryland Department of Transportation. His interests are in concrete materials, infrastructure performance modeling & life-cycle analysis, and computational simulation to mention a few.
- [4]  Experienced Engineering Manager with a demonstrated history of working in the government administration industry. Finished PhD courses in Vanderbilt University.
- [5]  Experienced Director of Infrastructure with a demonstrated history of working in the higher education industry.